Juni Khyat
(UGC Care Group I Listed Journal)
ISSN: 2278-4632
Vol-13, Issue-06, June 2023

An Integrated Hybrid Power Supply for Distributed Generation Applications Fed by Nonconventional Energy Sources

Dr.S. Selvakumar Raja[1], Mr.B.Mahendar[2], Mr.M.Balu[3], Mrs.M.Srujana[4]
[1]Principal & Professor, ECE Department, Kakatiya Institute of Technology and science for Women, Nizamabad, Telangana, India. kitswnzb@gmail.com
[2]Associate Professor, EEE Department, Kakatiya Institute of technology and science for women, Nizamabad, Telangana, India.
[3,4]Assistant Professor, EEE department, Kakatiya Institute of technology and science for women, Nizamabad, Telangana, India.

ABSTRACT

The use of photovoltaic (PV) and power cell (FC) power sources in an unique cold-blooded integrated architecture that is appropriate for distributed power generation operations is proposed. It serves as an uninterruptible power source that can always provide the grid with a certain minimum amount of electricity. The FC section (block) serves as the power source and an only supply fault power while PV is employed as the primary power source and operates close to the maximum power point (MPP). A novel "integrated" technique eliminates the requirement for separate conventional DC/DC boost motor stages necessary for PV power processing, as well as the necessity for specific communication between two sources for collaboration. A detector and the number of bias factor reads are both decreased. The voltage drop across the PV material is reduced when the FC power supply is connected in parallel with the PV power supply, which also enhances the quality of the energy sent to the grid. Another benefit is that a tiny quantity of PV electricity can actually be fed into the grid (for instance, when there is little solar radiation). On the other side, the extra energy is directed to extra tasks like electrolysis, resulting in the best possible utilisation of the energy sources. The proposed system also has cheap cost, a small footprint, and excellent dependability as benefits. This qualifies the system for modular construction and "plug and play" operation. All theoretical, simulation, and experimental results of this investigation are presented.

Index Terms—Buck-boost, distributed generation, fuel cell, grid-connected, hybrid, maximum power point tracking (MPPT), photovoltaic.

I. INTRODUCTION

In the past, centralized power products were preferred. Power plants are always located under populated areas and have access to energy and reaction forces. This reduced transportation costs while avoiding implicit (energy) pollution in high traffic areas. Voltage gestures despite similar bugs like resistive (i2R) losses (caused by energy transfer over long lines).

Problems, power quality issues, and deployment limitations have made analog systems relatively common these days, requiring more and more power, making these centralized power plants impractical. Distributed generation systems (DGS) were developed as a result of a shift in emphasis towards "natural" generation (and consumption) [1]–[4]. There may or may not be a wind resource. Possibly more dependable alternatives to power cells exist, but they come at a cost. A source is necessary. The Mongrel Distributed Generation Called System HDGS [5]-[7] is a comparable system that combines many energy sources into a single DG system. For HDGS functioning, the combination of PV and FC sources creates a solid bracket with favorable characteristics [6]. Of course, ultracapacitors or batteries (preferred due to their high energy viscosity) must be used to make up for the FC's poor response time [8], [9]. Here is a brief summary of the literature on HDGS systems. The HDGS structure depicted in Figure 1. was first suggested by Tam and Rahman (10) in early work. It is made up of two inverters that operate similarly and are linked to the grid by a single multi-winding the stepper motor.

This advanced technique has the disadvantage of not using Maximum Power Point Shadowing (MPPT), which prevents it from making optimum use of the

ISSN: 2278-4632
Vol-13, Issue-06, June 2023

available sources. The system was later enhanced by Ro and Rahman [11] by adding a dual-loop controller with MPPT. A multi-input, bidirectional DC-DC motor arrangement utilising a combination of DC connections and alluring couplings was proposed by Tao et al. [12]. High gain capability and galvanic isolation are provided by this setup. With a new DC/AC inverter stage to supply AC loads, it still has several power processing stages. As a result, we require a lot of biases. Another HDGS arrangement with PV, FC, and battery power sources that can satisfy the switching requirements at the end of charge was proposed by Monai et al. [13]. To ensure proper cargo allocation among coloured sources, the authors proposed a modified Eulerian moving average model. The suggested system is appropriate for high performance kilometre or standalone operation. A hybrid system that generates hydrogen using excess energy from renewable resources was proposed by Agbossou et al. [14]. Another useful technique is suggested by Rajashekara [15], who uses PV and FC sources for space operations. Additionally, people are becoming more aware of the need of preserving pristine landscapes and the potency of quickly decreasing fossil resources.

Cap AND Rahman (5) projected the HDGS structure shown in Fig. 1.1 in a previous study (a). It consists of two inverters operating identically, each connected to the grid via a multi-winding motor. Maximum Socket Dogging (MPPT) is not suitable for this complex topic, so getting to the source quickly is difficult. Rahman and Artificial Voice complemented this strategy by presenting his two-loop MPPT controller. DC link and ornate coupling were used to create a double-sided multi-input DC/DC motor design by Tao et al. Galvanic isolation and high gain capacity are features of this technology. It utilizes a brand-new DC/AC electric motor stepper powered by AC ground and numerous power processing stages. Therefore, a wide selection of outfits is required.

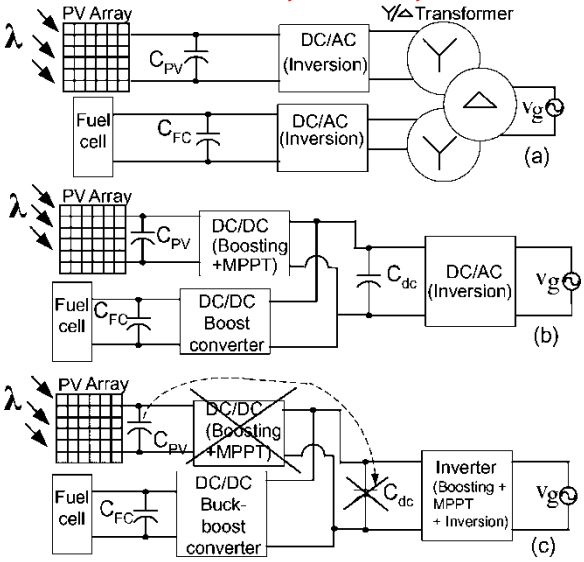

Fig. 1. (a) Two H-mass inverters in a conventional multilayer topology (b) Rearranged topology with a single H-mass inverter (c) Proposed topology for sun isolation (suns)

Another his HDGS setup with PV, FC and battery power was proposed by Monai et al. (13) Considered suitable to meet unstable charge termination criteria. To properly split the cargo among the colorful sources, the authors created a moving average divination model of the modified Euler type. The suggested system might be a good choice for disconnected or mileage-based mains operation. A hybrid system presented by Agbossou et al. leverages the extra energy generated by renewable tillers to generate a minimal number of 1s. In addition to his PV and his FC sources, Rajashekara suggests another profitable method of primal operations. The system stylishly harnesses the sun's energy and electrolyzes excess energy to create a tiny number one. Balenciaga et al. studied another of his HDGS systems that combined wind, PV, and battery sources. We are talking about a control system that maintains both the battery's state of charge and its need to be charged. Blaabjerg et al. In our 2016 paper, we published a detailed study of colorful grid synchronization and control strategies used in HDGS systems. Real-world examples of HDGS systems FC, PV, and wind energy-based publications have also been made.

The recently proposed mixer-battery employs PV and FC feeding systems and separate step-up DC-DC transformers with a complex inverter stage for each of the two power sources. The DC-DC motor stages are made to increase low voltages for FC and PV. The MPPT is likewise managed by the PV side motor. To avoid restricted operation, his PV-side DC-DC motor in this system should be turned off during very low solar irradiance. As a result, generation from PV sources is not used in low power situations. While this may be fine for

ISSN: 2278-4632
Vol-13, Issue-06, June 2023

high power operation, it can cause problems in domestic or medium power installations. Still, if his DC-DC motor function on the PV side is connected to the reversing step as shown in the figure.

The maturity of HDGS systems using H-mass inverter topologies to manage grid connections now requires high DC link voltages at the heavy power frequency motors or inverter inputs in question. This work proposes intertwined results using a special setup as depicted in Fig. 1.(c) for PV-FC-grounded HDGS. The suggested solution avoids the necessity for high DC voltage at the inverter input and saves Plutocrat in high voltage buffer capacitors by utilising an inverter with boost capability. The next parts go into further design elements, operational suggestions, control systems, modelling, and experimental findings.

II. PROPOSED SYSTEM

Using an MPPT inversion-based buck-boost inverter topology, boost and buck voltage capabilities, the suggested topology is based on this (dc-ac). The primary idea of the recommended integrated layout is shown in Fig. 2. A detailed representation of Figure 2.(a) and an application example are shown in Figure 2(b) (electrolysis).

A combination of PV and FC energy sources are used to power the system. As seen in the illustration, the FC source interfaces with the inverter via a buck-boost type dc-dc converter, while the PV source feeds the inverter directly through a buffer capacitor, CPV. As seen in the image, a second block is put across the CPV source to direct any surplus power through a buck-boost type dc-dc converter (Preq). The main energy source of the suggested system, the PV, is continuously tuned to follow the MPP while supplying the grid with the necessary quantity of electricity.

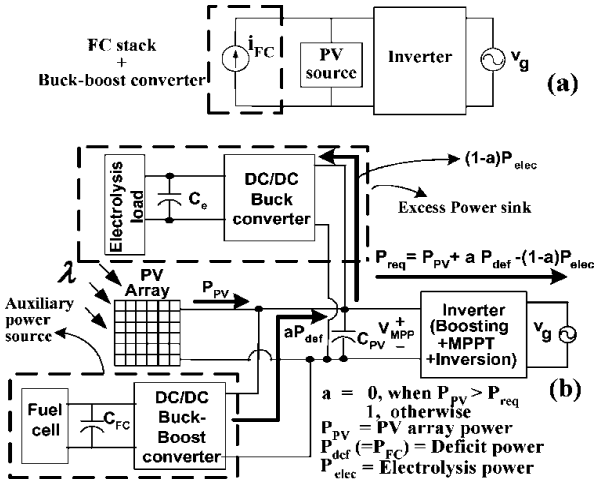

Fig. 2. Proposed configuration (a) Block diagram illustrative of the fundamental idea (b) Detailed view and electrolysis

A power source similar to a PV power supply is an FC power supply with a DC-DC motor of the buck-boost type. When there is little or no solar radiation, only used as a backup for PV sources. FC only increases the network's redundant energy supply. Contrarily, the "waste energy" generated by PV sources is changed and put to use for extracurricular activities, much like electrolysis is utilized to create hydrogen. FC sources can also store hydrogen for later use.

This makes the system very cost-effective and the cash registers are used optimally. As a result of the discussion above, the proposed system works in one of three ways:

Only utilize PV mode in mode I (only PV provides power)

Hybrid setting in Mode-II (both PV and FC provide power)

Supports only Mode-III FC mode (only FC provides power). A list of these functional modes can be found in Table I.

Table I
Proposed HDGS System Operating Modes

Operating mode	Applicable condition	Active sources	Active power converters
I	$P_{ex}=P_{PV}-P_{req}\geq 0$	Only PV	Buck*(for $P_{ex}\geq 0$)
II	$P_{def}=P_{req}-P_{PV}\geq 0$	PV and FC	Buck-Boost
III	$P_{PV}\approx 0$	Only FC	Buck-Boost

The expected composition offers a variety of interesting druthers due to their unique nature integrated with hybrids, as posted below.

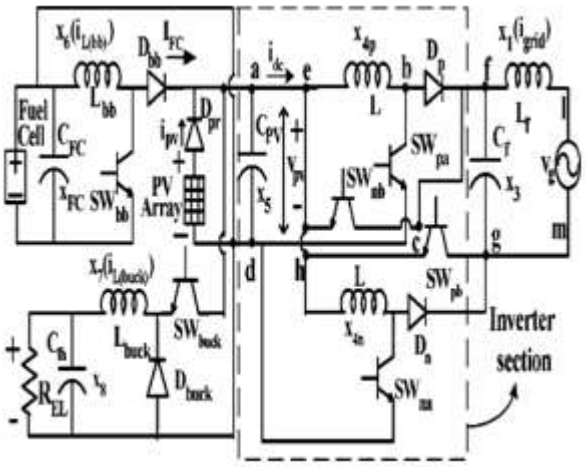

Fig. 3. The corresponding state variables are represented in the schematic diagram of the proposed integrated configuration of the mixed distributed generation system.

ISSN: 2278-4632
Vol-13, Issue-06, June 2023

1. Eliminates the need for the swept converter stage shown in Figure 2 when learning PV power.
2. One CPV and two condensers (Figure 2(a)), only one is required.
3. Due to dynamic environmental conditions, using similar FC can reduce PV voltage fluctuations.
4.As a result, the power in the network oscillates less. A better performance intensity profile is terminal growth (23). Four. Reducing PV voltage harpoons and dips increases the effectiveness of MPPT.
5. The square of the measured electromechanical voltage (Cdc) he calculated with MPPT and power manipulation and is awarded separately. Within a planned system, the agency (or DC-CPV with each PV array in a 5" by 4" two-stage system) is usually placed directly across from the PV outstation. .2(b)). So one device is enough.
6. Eliminates the need for new equipment to communicate and coordinate between different sources to achieve optimal storage and application of requested energy (24).
7. The FC section serves as the power source for the voltage quantities in question thanks to a special arrangement that connects the vestibule's PV and FC sources. The PV voltage that is required for operation near to the MPP is now easy to adjust.
Anticipated, his eighth design could provide maneuverable, inexpensive, and safe positional response for HDG operations.

III. CONTROL SYSTEM

A. MPPT algorithm and control scheme

To enable the necessary power input, the modulation indicator M of the grid-connected SPWM inverter is modified. The available power is determined by the observed MPP due to this

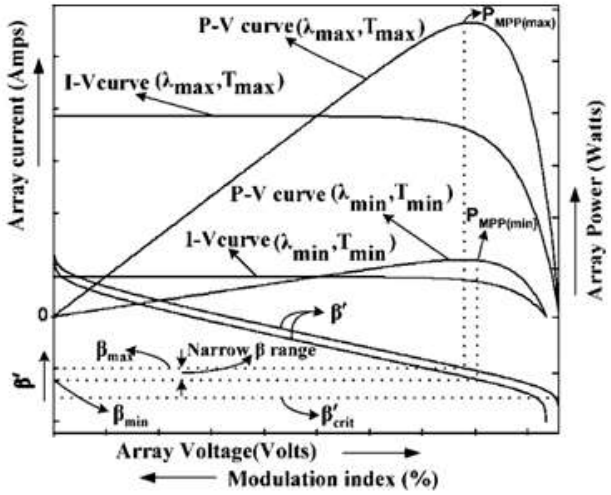

Fig. 3. I-V and P-V properties of the PV array, as well as a curve

The value of M is determined using the MPPT algorithm. Several MPPT variations are offered upon request. Small incremental modifications in the modulation indicator that are insufficient to balance input and relationship performance across CPV lead to poor late shadowing results. Fixed small incremental changes in modulated power entering the system. Common MPPT styles such as incremental conductance approaches and hill climbing are therefore empty. This creates an open circuit condition at the PV operating point, similar to the PV source in use (OCC). Furthermore, modulation shift indexing can only be performed at the start of the mains voltage. If the MPPT algorithm is slow, the PV power may be underutilized. Borrowing a rapid-fire MPPT system is essential to overcome the drawbacks of the slow approach.

For certain operations, the rapid-fire MPPT system, also known as the "" system, is modified as needed. This design is based on the observation that when the MPP shifts from PMPP (max) to PMPP, the values of intermediate variables defined only under MPP conditions change in the bands marked by arrows (max, min) (min). Based on as a result, I am. Figure 2 shows the change in temperature range (Tmax to Tmin) and total solar radiation. β is a subset of βj that fits all P-V upwind points containing the MPP. β is the result of the MPP condition
∂ P/ dV = 0 and is given by

$$\beta = In(-I_o * c) = In\frac{I_{PV}}{V_{PV}} - c * V_{PV} \quad (1)$$

Io refers to the diode's reverse saturation current. As a result, changing the operational point to narrow MPP bands is simple when tracking in large iteration steps. Indirect methods for regulating the operational voltage include (OV).

Mmin and Mmax stand for the modulation indicator's inner and outer values, respectively. Keep in mind that when the amount of PV power generated is very low, the PV array's CPV capacitance, which helps balance the system, is reasonable for the MPP algorithm program and the value of "M" becomes very important please give me. If FC continues to match insufficient power between input power and operating power, an imbalance can occur and the voltage across CPV will rise. As a result, the solar plant terrorist group may also relocate him to the OCC. In fact, even with high or normal increases in solar irradiance, the array can remain in OCC and the system can keep using FC to get the power it requires. We changed the algorithm programme such that the PV array voltage typically corresponds just to the critical voltage to prevent a situation like this (Vcrit.H). below the PV array's VOC.

ISSN: 2278-4632
Vol-13, Issue-06, June 2023

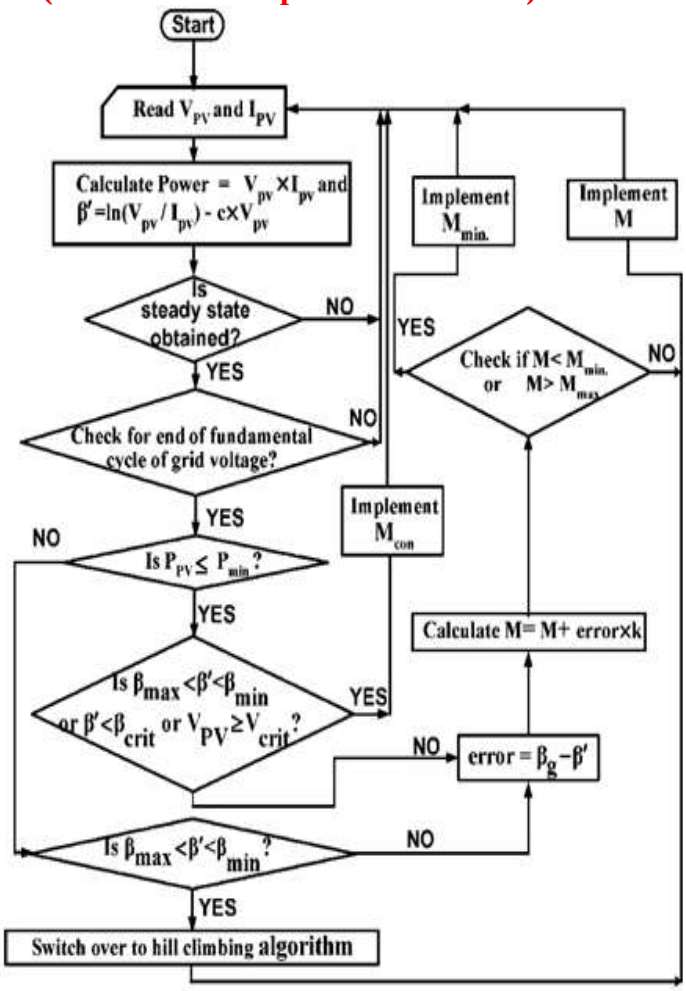

Fig. 4. Algorithm used in flow chart of projected HDGS topic MPPT program

IV. CIRCUIT OPERATION AND ANALYSIS

Along with the electrolysis application, Fig. 2 shows the full circuit architecture for the recommended arrangement. The suggested topology in chapter II is divided into three parts, which are represented in Fig. 2:

1. The electrical conversion part of a network connection.
2. Buck-boost DC-DC forming tool for FC power supply
3 A humped DC-DC motor that can learn to use redundant solar power for electrolysis operation. Two buck-boost transformers coupled in a controllable network form an electric motor device. Each trial (SWpa and SWpb or SWna and SWnb) uses a half cycle of force stress. Back to back (25) as shown in Figure 2. Two sets of switches are used to turn SWpb (or SWnb) on continuously and the opposite side SWpa (or SWna) on for the entire frequency, positive (or negative) half cycle, and supply voltage. Region modulation is actively performed by the indirect function (SPWM).

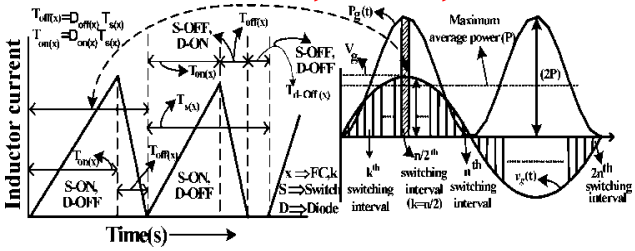

Fig .5. An inductor current waveform in discontinuous conduction mode is made up of three periods.

TABLE II:

Current pathways and appliance status during the grid voltage's positive half-cycle

State of the device			Corresponding State equations *	Active current Path(s)
SW_{p1}	SW_{p2}	D_1		
ON	ON	OFF	$i_{dc} = C_{PV} x'_5 + x_{4p}$; $x_5 = L x'_{4p}$ $C_f x'_3 + x_1 = 0$; $x_3 = (L_f) x'_1 + v_g$	a-b-c-d-a; f-l-m-g-f
OFF	ON	ON	$i_{dc} = C_{PV} x'_5$; $x_3 = (L_f) x'_1 + v_g$ $-x_3 = L x'_{4p}$; $C_f x'_3 + x_1 = x_{4p}$	e-f-g-h-e; f-l-m-g-f
OFF	ON	OFF	$i_{dc} = C_{PV} x'_5$; $C_f x'_3 + x_1 = 0$ $x_3 = (l_f) x'_1 + v_g$; $0 = l x'_{4p}$	f-l-m-g-f

The squaring converter produces a high-quality adaptation of the current waveform to the grid (DCM) when used in spasitic current mode. The device is made to operate efficiently in drag mode (continuous current mode (CCM) and DCM limited) when the mains are supplied with two times the usual average power. increase. The natural medicine and DCM surgical approaches are shown in Figure 3. Energy is stored in the electrical device "L" when SWpa is activated. When SWpa turns off, this stored energy is transferred to capacitor "Cf." An atrium's on/off time modulation that is highly distorted also affects the current that is sent to the grid. Table II displays the active current paths and associated equations of state for the operation of the electric motor during the positive half-cycle of the supply voltage vestibule. Gestures and judgements performed during the negative half-wave of the mains voltage are accurate when electric motors operate in DCM. Each high frequency switching cycle entirely transfers energy from the buck-boost electrical gadget to the grid. Assuming that the frequency of change is an integer multiple of the line harmonics, the line voltage is divided into '2n' factors or intervals for each period (fs(= 1/ Ts) = 2n fg(1/ Tg)). Every one of these epochs involves the transmission of a certain amount of energy. Assuming a constant line voltage, the duty cycle DON(k) for the kth (k=1,2,...,n) lamp cycle is given by $D_{ON(k)} = M \times \sin(\pi \times (k/n))$, where, M =Vsin /Vtri (1)

ISSN: 2278-4632
Vol-13, Issue-06, June 2023

$$E_{k(inv)} = \frac{L}{2} * \left(\frac{V_{PV}}{L}\right)^2 * \left(T_s * M * sin\left(\pi * \frac{k}{n}\right)\right)^2 \quad (2)$$

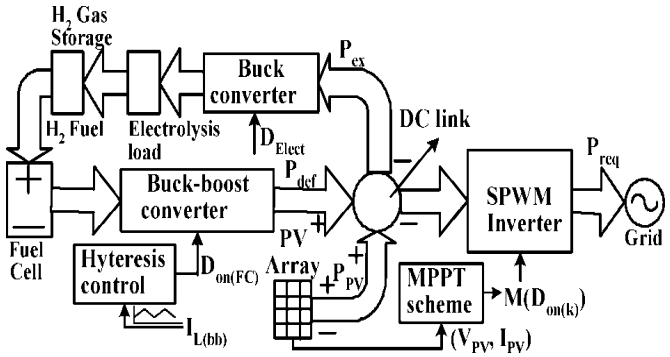

Fig. 6. A simplified representation of the projected representation of the configuration's control variables for HDGS.

The direction of inflow within the system is indicated by an arrow next to the 4. intermodal icon Operation conversion and shutdown. The Mode 1 M and VPV values determine the amount of power sent to the grid, but the M, VPV, and DON(FC) delivered to the grid throughout the plant depend on the M Mode II values. From III, depending on the value Equations (3) and (5) give the values for VPV and M set. An operating theme governs the value of power delivered by the VPV's electric motor set. The (acclimated) force of the plant from FC (controlled by DON (FC)) m to the MPPT demand is not strictly a DC force and therefore cannot be sprinkled with the FC force. As shown in Figure 4, the problem of natural power influx, and thus the abundant power Pex generated by managed variable PV power, is amortized for use in the projected HDGS configuration. Electrolytic operation with a step-down transformer. The energy cell, hydrogen, will be stored to provide Pdef from electrolysis at a later date and will be used by the overall operational theme corresponding to three complementary freelance operational circles.

1. Motorized operation by SPWM combined with MPPT
2. FC feature operation of a DC-DC motor.
3 unusual high-power operations (DC-DC Buck Motor Control)

The proposed system's overall control mechanism and the sense control verity table are shown in Figure 4. Preq>PPV causes the logic manager to turn off pex interesting control of electrolysis and radio operation of FC's ex-following pdef. The opposite is also true. The Sense controller coordinates individual overpowered and underpowered controllers that are never on at the same time. Now let's take a closer look at the two controls.

1) SPWM management of transformers associated with MPPT

The electric motor acts as a victim of his SPWM technology, injecting curvilinear currents into the grid in all three modes of operation.

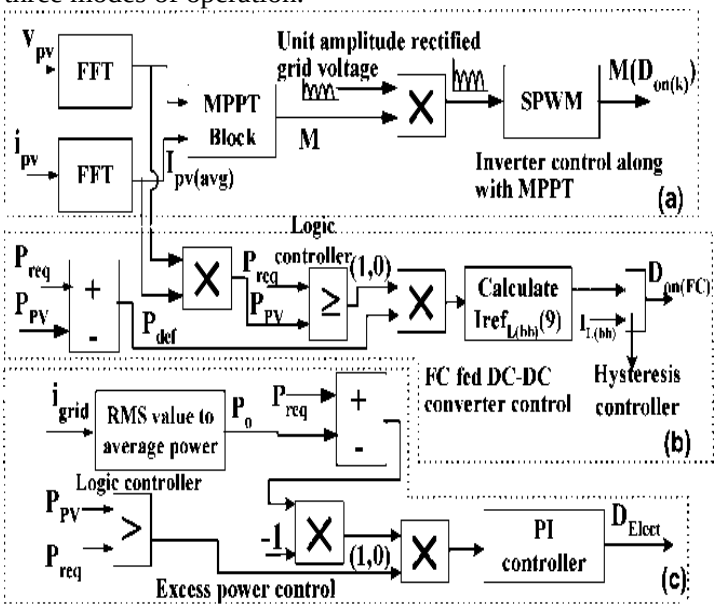

$P_{req} \geq P_{PV}$	FC controller	Electrolysis Controller
1	1	0
0	0	1

(d)

Fig. 7. demonstrates the complete control architecture used in the suggested system. Control of the FC side buck-boost converter; (A) control for inverters calculated in the MPPT block the Buck Converter's control. (d) The truth tables of the logic controllers.

A. Mathematical logic controller

LoftiA. Zade introduced a very different and subtle sensation. The state of the natural property value of the calculated sense sphere unit must also be 1 (ON) or 0 (OFF). The ability of mathematical meaning to accept just two or new values between true and false sets it apart from symbolic meaning. It just accepts true or false, unlike symbolic meaning. We can make informed decisions from ambiguous and ambiguous facts with the aid of mathematical sense. The multi-level salient H-bottom inverter that uses a fuzzy logic controller (FLC) to accomplish VR is depicted in Figure 8. In this instance, a reference voltage (Vref), or the preferable voltage produced by the inverter in accordance with grid norms, is compared to the grid voltage (Vo) of the 15-position inverter. The input parameters for FLC are the rate of change de/dt and the posterior error e = Vref Vo. There are 5 substantial block sets in FLC. They are fuzzifiers, defuzzifiers, reasoning systems, rulebases, and databases. In class functions, fuzzing transforms the input data into class degrees.

ISSN: 2278-4632
Vol-13, Issue-06, June 2023

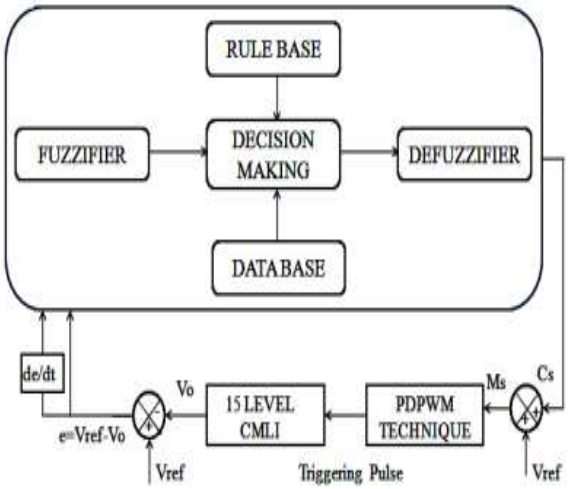

Fig. 8. Fuzzy logic control structure

The appropriate gating signals are delivered to the semiconductor switches in the inverter power circuit by the modulating signal Ms required for PWM (pulse width modulation) generation. The problem (membership function) is formulated using the error and its derivative MF. Figure 4.5 shows the MF for the wrong signal. N, P, and Z represent negative, positive, and zero, respectively, in this figure. The letters B, M, S, and E, respectively, stand for big, medium, tiny, and error. The derivative of the error signal for the fuzzy logic controller input and its MF is shown in Figure 8.

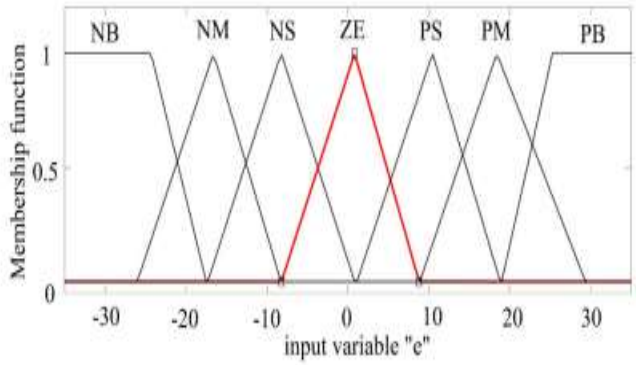

Fig. 9. Function for error signal participation

A membership function-derived reference signal is the outcome of fuzzy logic, as depicted in Figure 9. Table 2 shows a rule matrix surrounded by a rule table with one output and two inputs (the error and its derivative signal). signal for referencing The defuzzification procedure is then used to convert the fuzzy value into a crisp value. The conversion (COG) was done using the Centre of Gravity method. The input error, its derivative, and the output reference signal are all shown in three dimensions in Figure 4.6. The crucial task is to adjust the controller gains in order to achieve the desired result.

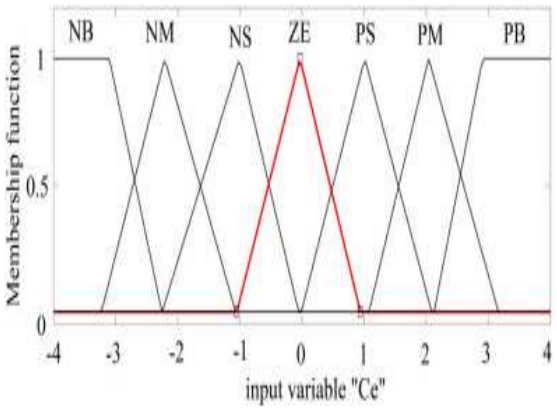

Fig. 10. MF for the change in an error signal

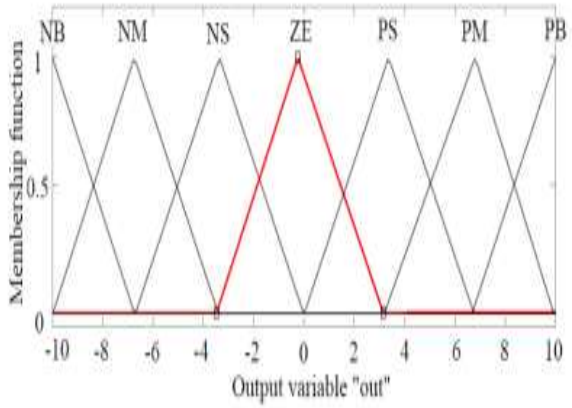

Fig. 11. MF for the reference output

TABLE III
FLC rule matrix

e / Ce	NB	NS	NM	ZE	PB	PS	PM
NB	PB	PB	PB	PB	ZE	PM	PS
NS	PB	PM	PB	PS	NM	ZE	NS
NM	PB	PB	PB	PM	NS	PS	ZE
ZE	PB	PS	PM	ZE	NB	NB	NB
PB	ZE	PS	NS	NB	NB	NB	NB
PS	PM	ZE	PS	NS	NB	NM	NB
PM	PS	NS	ZE	ZE	NM	NB	NB

ISSN: 2278-4632
Vol-13, Issue-06, June 2023

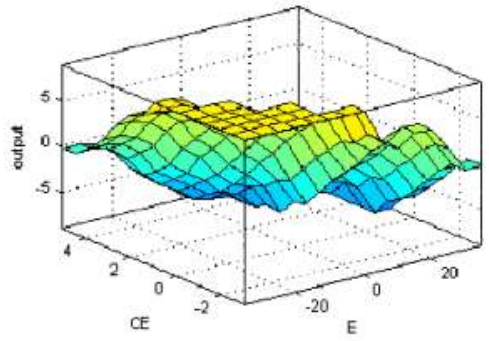

Fig.12. D visualization of Fuzzy rules

V. SIMULATION RESULTS

Simulation results for the main HDGS configurations are shown in Figure 13. No excessive power operation. Results for the specified lambda region that correspond to low, medium, and high values. Note that FC delivers full Preq (= 500 W) from t = 0 s as soon as it becomes negligible. As the value of Forward t = 1.2s λ increases, so does the PV power. Considering PPV(t) PFC(t) = Preq mechanically reduces the decision power of FC. The PV power operates close to the MPP, making optimal use between the two sources. The value is further enhanced, and PV is also modified over his Preq, before t = 3 s. Reduced to 0% PFC. As there is no power diversion, redundantly generated PV power is also delivered to the grid. In any case, note that the designed system can deliver the declared performance (Preq) in all three modes, as shown in the image. Preq is also maintained during fast transitions between the two modes.

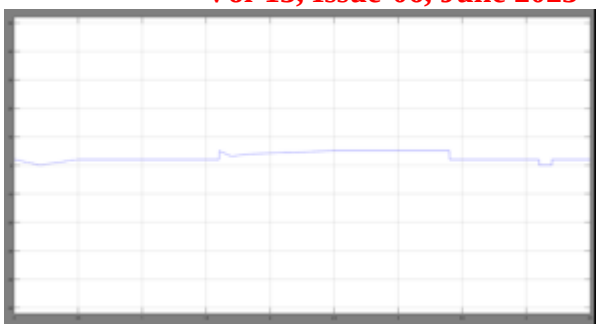

(a)

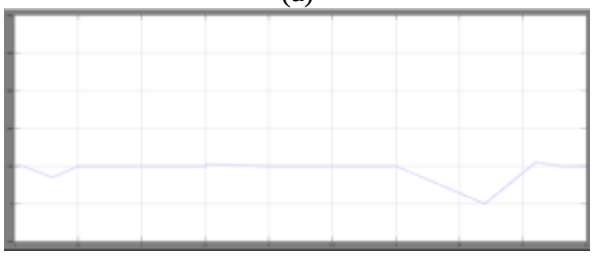

(b)

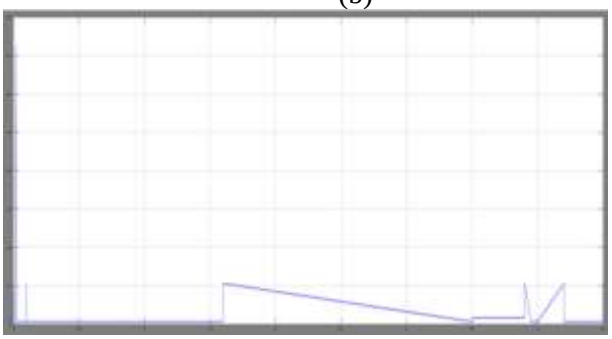

(c)

Fig. 14. The results of the simulation Without a concurrent FC source and PV source, the suggested HDGS system's performance is evaluated.

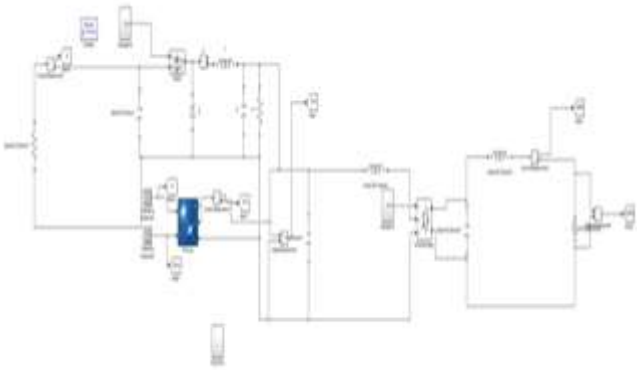

Fig. 13. Simulation model without FC

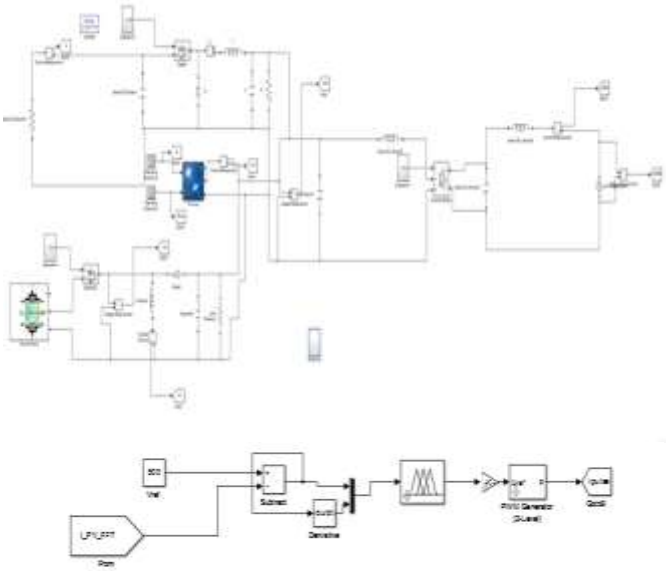

Fig.15. Simulation mode solar with FC

ISSN: 2278-4632
Vol-13, Issue-06, June 2023

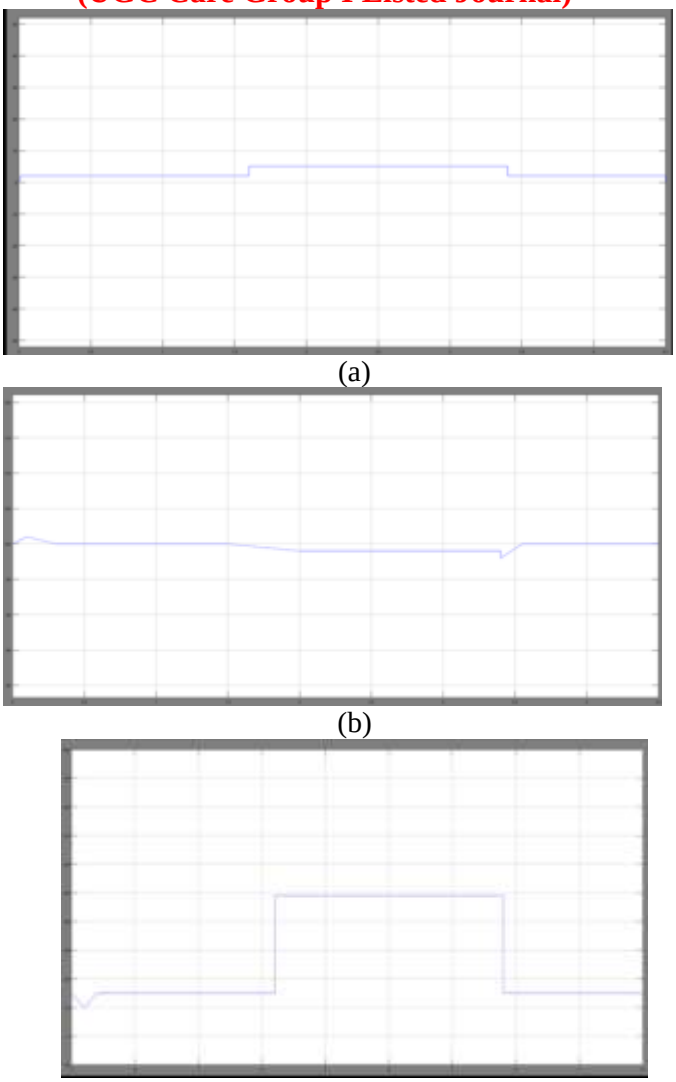

Fig. 16. Problems of Simulation Performance Evaluation of Proposed HDGS System Equipped with FC Power Supply and PV Power Supply Simultaneously

Surplus PV power (Pex) is diverted using a step-down motor for electrolytic operation, as shown in the redundant power control simulation results in Figure 5.4. This avoids the increase in Mode I grid voltage that would be affected by adding redundant power to the system. Additionally, Preq is continuously fed to the grid from a PV system near his MPP. A small increment of 7.9 s in ambient conditions indicates that the tap power increases accordingly when the PV array is operating in his MPP.

To demonstrate the need to connect an FC light source similar to a PV light source, simulations were performed for irradiance step changes with and without an FC light source in the circuit. Present the findings. FC was established to improve the MPPT process and increase system efficiency by reducing voltage and current droop in PV arrays. Additionally, FC reduces the total harmonic distortion (THD) of the grid current during transients. A working 300W prototype system was set up to test the simulation results and other theoretical findings.

The performance of the FC power supply with left and ultra capacitors is comparable to that of the rigid DC power supply, so the tests were performed using the rigid DC power supply rather than the power cell source (4). CPV=2000F, L=310H, Cf=2.2F, Lf=3.25mH, Lbb=0.7mH, Lbuck=2mH are the element values of the prototype. The power diode used is CSD20060 and the controllable power bias MOSFET used is IRFP460. Also, the conditions are VPV 90V, Vg=140V, Vg=50V. A TMS320LF2407 digital signal processor was used to implement the control system shown in Figure 4. A DSP controller was used to enable the MPPT approach to determine the mean values of the recorded PV voltages and PV currents by a quick Fourier transform. It was also used to encode Po, Iref L(bb), and other functions. LEM current detectors are used to record iPV, iL(bb) and grid current values. A TL084 JFET input stage op amp with high input impedance, bandwidth and slew rate was used to apply PI and hysteresis control.

VI. CONCLUSION

The default topology is Grid Coupling, which is compact and easy to work with. Analysis, operational ideas, and design methodologies were provided. This topology uses PV and FC cold-blooded power supplies. PV acts as the main source and FC acts as the backup source to serve source queries. It improves network power quality and reduces the distance between FC power supplies and MPPs. The system performance with and without FC blocks is compared in Table IV. The advantage of the suggested setup is the direct connection of the PV power source to the inverter. FC serves as a power source as well. PV can function in MPP with a wide range of solar isolation since FC is not a strictly DC power supply, restricting the best possible utilization of the energy source. The effectiveness of mode 1 (85-90) in the proposed system is higher than that of modes 2 and 3 (80-85). Analysis of the results shows that FLC gives better results for VR, taking into account the vibrations in signaling the photovoltaic PV.

REFERENCES

[1] J. Kabouris and G. C. Contaxis, “Optimum expansion planning of an unconventional generation system operating in parallel with a large scale network,” IEEE Trans. Energy Convers., vol. 6, no. 3, pp. 394–400, Sep. 1991.

[2] P. Chiradeja and R. Ramakumar, “An approach to quantify the technical benefits of distributed generation,” IEEE Trans. Energy Convers., vol. 19, no. 4, pp. 764–773, Dec. 2004.

[3] Y. H. Kim and S. S. Kim, “An electrical modeling and fuzzy logic control of a fuel cell generation system,” IEEE Trans. Energy Convers., vol. 14, no. 2, pp. 239–244, Jun. 1999.

ISSN: 2278-4632
Vol-13, Issue-06, June 2023

[4] K. N. Reddy and V. Agarwal, "Utility interactive hybrid distributed generation scheme with compensation feature," IEEE Trans. Energy Convers., vol. 22, no. 3, pp. 666–673, Sep. 2007.

[5] K. S. Tam and S. Rahman, "System performance improvement provided by a power conditioning subsystem for central station photovoltaic fuel cell power plant," IEEE Trans. Energy Convers., vol. 3, no. 1, pp. 64–70.

[6] R. Kyoungsoo and S. Rahman, "Two loop controller for maximizing per- formance of a grid-connected, photovoltaic fuel cell hybrid power plant," IEEE Trans. Energy Convers., vol. 13, no. 3, pp. 276–281, Sep. 1998.

[7] F. Valenciaga and P. F. Puleston, "Supervisor control for a stand-alone hybrid generation system using wind and photovoltaic energy," IEEE Trans. Energy Convers., vol. 20, no. 2, pp. 398–405, Jun. 2005.

[8] N. Kato, K. Kurozumi, N. Susuld, and S. Muroyama, "Hybrid power- supply system composed of photovoltaic and fuel-cell systems," in Telecommun. Energy Conf., Jpn, Oct., 2001, pp. 631–635.

[9] T. Senjyu, T. Nakaji, K. Uezato, and T. Funabashi, "A hybrid power system using alternative energy facilities in isolated island," IEEE Trans. Energy Convers., vol. 20, no. 2, pp. 406–414, Jun. 2005.

[10] Y. M. Chen, C. S. Cheng, and H. C. Wu, "Grid-connected hybrid PV/wind power generation system with improved dc bus voltage regulation strategy," in Proc. IEEE APEC, 2006, pp. 1089–1094.

[11] W. Gao, "Performance comparison of a fuel cell-battery hybrid power train and a fuel cell-ultra capacitor hybrid power train," IEEE Trans. Veh. Technol., vol. 54, no. 3, pp. 846–855, May 2005.

[12] H. Tao, A. Kotsopoulos, J. L. Duarte, and M. A. M. Hendrix, "Multi-input bidirectional dc–dc converter combining dc-link and magneticcoupling for fuel cell systems," in Proc. IEEE Conf. Ind. Appl., 2003, vol. 3, pp. 1136– 1142.

[13] T. Monai, I. Takano, H. Nishikawa, and Y. Sawada, "A collaborative operation method between new energy-type dispersed power supply and EDLC," IEEE Trans. Energy Convers., vol. 19, no. 3, pp. 590–598, Sep. 2004.

[14] K. Agbossou, M. Kolhe, J. Hamelin, and T. K. Bose, "Performance of a stand-alone renewable energy system based on energy storage as hydro- gen," IEEE Trans. Energy Convers., vol. 19, no. 3, pp. 633–640, Sep. 2004.

[15] K. Rajashekara, "Hybrid fuel-cell strategies for clean power generation,"
IEEE Trans. Ind. Appl., vol. 41, no. 3, pp. 682–689, May/Jun. 2005.